Time from quantum entanglement: An experimental illustration

Ekaterina Moreva,[1,2] Giorgio Brida,[1] Marco Gramegna,[1] Vittorio Giovannetti,[3] Lorenzo Maccone,[4] and Marco Genovese[1]

[1]*INRIM, Strada delle Cacce 91, I-10135 Torino, Italy*

[2]*International Laser Center of M.V. Lomonosov Moscow State University, 119991, Moscow, Russia*

[3]*NEST, Scuola Normale Superiore and Istituto Nanoscienze-CNR, Piazza dei Cavalieri 7, I-56126 Pisa, Italy*

[4]*Dipartimento di Fisica "A. Volta", INFN Sez. Pavia, Universitàà di Pavia, Via Bassi 6, I-27100 Pavia, Italy*

(Received 7 November 2013; published 20 May 2014)

In previous years several theoretical papers discussed if time can be an emergent property deriving from quantum correlations. Here, to provide insight into how this phenomenon can occur, we present an experiment that illustrates Page and Wootters' mechanism of "static" time [D. N. Page and W. K. Wootters, Phys. Rev. D **27**, 2885 (1983)], and Gambini *et al.* for subsequent refinements [R. Gambini *et al.*, Phys. Rev. D **79**, 041501(R) (2009)]. A static, entangled state between a clock system and the rest of the universe is perceived as evolving by internal observers that test the correlations between the two subsystems. We implement this mechanism using an entangled state of the polarization of two photons, one of which is used as a clock to gauge the evolution of the second: An "internal" observer that becomes correlated with the clock photon sees the other system evolve, while an "external" observer that only observes global properties of the two photons can prove it is static.

DOI: 10.1103/PhysRevA.89.052122 PACS number(s): 03.65.Ta, 03.65.Ud, 04.60.Ds, 42.50.Xa

One of the main aspects of the "problem of time"[1] [1–6] stems from the fact that a canonical quantization of general relativity yields the Wheeler–De Witt equation [7,8] predicting a static state of the universe, contrary to obvious everyday evidence. This is only a facet of the "problem of time," but similar aspects also occur in other approaches to quantum gravity [5]. A solution was proposed by Page and Wootters [9,10]: thanks to quantum entanglement, a static system may describe an evolving "universe" from the point of view of the internal observers. Entanglement between a "clock" system and the rest of the universe can yield a stationary state for an (hypothetical) external observer that is able to test it vs abstract coordinate time. The same state will be, instead, evolving for internal observers that test the correlations between the clock and the rest [9–14]. Thus, time would be an emergent property of subsystems of the universe deriving from their entangled nature: an extremely elegant but controversial idea [2,15]. Here we want to illustrate it by showing experimentally that it can be naturally embedded into (small) subsystems of the universe, where Page and Wootters' mechanism (and Gambini *et al.* subsequent refinements [12,16]) can be easily studied. We show how a static, entangled state of two photons can be seen as evolving by an observer that uses one of the two photons as a clock to gauge the time evolution of the other photon. However, an external observer can show that the global entangled state does not evolve.

I. THE PAW MECHANISM

Even though it revolutionizes our ideas on time, interpretation of Page and Wootters' (PaW) mechanism is easily summarized [9–11]: They provide a static entangled state $|\Psi\rangle$ whose subsystems evolve according to the Schrödinger equation for an observer that uses one of the subsystems as a clock system C to gauge the time evolution of the rest R. While the division into subsystems is largely arbitrary, the PaW model assumes the possibility of neglecting interaction among them writing the Hamiltonian of the global system as $\mathcal{H} = \mathcal{H}_c \otimes \mathbb{1}_r + \mathbb{1}_c \otimes \mathcal{H}_r$, where $\mathcal{H}_c, \mathcal{H}_r$ are the local terms associated with C and R, respectively [10]. In this framework the state of the "universe" $|\Psi\rangle$ is then identified by enforcing the Wheeler–De Witt equation $\mathcal{H}|\Psi\rangle = 0$, i.e., by requiring $|\Psi\rangle$ to be an eigenstate of $\mathcal{H}$ for the zero eigenvalue. The rational of this choice follows from the observation that by projecting $|\Psi\rangle$ on the states $|\phi(t)\rangle_c = e^{-iH_c t/\hbar}|\phi(0)\rangle_c$ of the clock, one gets the vectors,

$$|\psi(t)\rangle_r := {}_c\langle\phi(t)|\Psi\rangle = e^{-iH_r t/\hbar}|\psi(0)\rangle_r, \tag{1}$$

that describe a proper evolution of the subsystem R under the action of its local Hamiltonian H_r, the initial state being $|\psi(0)\rangle_r = {}_c\langle\phi(0)|\Psi\rangle$ (see Fig. 1). Therefore, despite the fact that globally the system appears to be static, its components exhibit correlations that mimic the presence of a dynamical evolution [9–11].

Two main flaws of the PaW mechanisms have been pointed out [2,15]. The first is based on the (reasonable) skepticism to accept that quantum mechanics may describe a system as large as the universe, together with its internal observers [11,12]. The second has a more practical character and is based on the observation that in the PaW model the calculations of transition probabilities and of propagators appear to be problematic [2,11]. An attempt to fix the latter issue has been discussed by Gambini *et al.* (GPPT) [12,16] by extending a proposal by Page [11] and invoking the notion of "evolving constants" of Rovelli [17]. It will be analyzed in detail in the following section.

In this work we present an experiment which reproduces the basic features of the PaW and GPPT models. In this section we consider the PaW model. It is realized by identifying $|\Psi\rangle$ with an entangled state of the vertical V and horizontal H polarization degree of freedom of two photons in two spatial modes c,r, i.e. (see Sec. III),

$$|\Psi\rangle = \frac{1}{\sqrt{2}}(|H\rangle_c|V\rangle_r - |V\rangle_c|H\rangle_r), \tag{2}$$

[1]Quid est ergo tempus? si nemo ex me quaerat, scio; si quaerenti explicare velim, nescio [1].

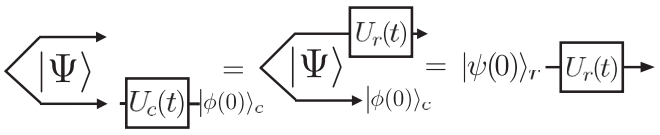

FIG. 1. Gate array representation of the PaW mechanisms for a CR noninteracting model. Here $U_r(t) = e^{-iH_r t/\hbar}$ and $U_c(t) = e^{-iH_c t/\hbar}$ are the unitary time evolution operators of the clock C and of the rest of the universe R, respectively. $|\Psi\rangle$ is the global state of the system which is assumed to be an eigenstate with null eigenvalue of the global Hamiltonian $H = H_c + H_r$ (see text).

and enforcing the Wheeler–De Witt equation by taking $\mathcal{H}_c = \mathcal{H}_r = i\hbar\omega(|H\rangle\langle V| - |V\rangle\langle H|)$ as local Hamiltonians of the system (ω being a parameter which defines the time scale of the model)[2]. For this purpose rotations of the polarization of the two photons are induced by forcing them to travel through identical birefringent plates as shown in Fig. 2(a). This allows us to consider a setting where everything can be decoupled from the "flow of time," i.e., when the photons are traveling outside the plates.

Although quite simple, our model captures the two, seemingly contradictory, properties of the PaW mechanism: the evolution of the subsystems relative to each other, and the staticity of the global system. This is achieved by running the experiment in two different modes [Fig. 2(a)]: (1) an "observer" mode, where the experimenter uses the readings of the clock photon to gauge the evolution of the other; by measuring the clock photon polarization he becomes correlated with the subsystems and can determine their evolution. This mode describes the conventional observers in the PaW mechanism; they are, themselves, subsystems of the universe and become entangled with the clock systems so that they see an evolving universe; (2) a "super-observer" mode, where he carefully avoids measuring the properties of the subsystems of the entangled state, but only global properties; he can then determine that the global system is static. This mode describes what an (hypothetical) observer external to the universe would see by measuring global properties of the state $|\Psi\rangle$. Such an observer has access to abstract coordinate time (namely, in our experimental implementation he can measure the thickness of the plates) and he can prove that the global state is static, as it will not evolve even when the thickness of the plates is varied. In observer mode [Fig. 2(a), pink (light gray) box] the clock is the polarization of a photon which has a dial with only two values, either $|H\rangle$ (detector 1 clicked), corresponding to time $t = t_1$, or $|V\rangle$ (detector 2 clicked), corresponding to time $t = t_2$. [Here $t_2 - t_1 = \pi/2\omega$, where ω is the polarization rotation rate of the quartz plate, since the polarization is flipped in this time interval.] The experimenter also measures the polarization of the first photon with detectors 3 and 4. This last measurement can be expressed as a function of time (he has access to time only through the clock photon) by considering the correlations between the results from the two photons: the time-dependent probability that the first photon is vertically polarized (i.e., that detector 3 fires) is $p(t_1) = P_{3|1}$ and $p(t_2) = P_{3|2}$, where $P_{3|x}$ is the conditional probability that detector 3 fired, conditioned on detector x firing [experimental results for the observer mode are presented in Fig. 3(a)]. This type of conditioning is typical of every time-dependent measurement; experimenters always condition their results on the value they read on the laboratory's clock (the second photon in this case). The experimenter has access only to physical clocks, not to abstract coordinate time [10,17,18]. In our experiment this restriction is implemented by employing

[2]It may be worth noticing that this state is analogous to the spin singlet state [9,10]. In this case the local Hamiltonians then correspond to local spin (σ_y) rotations.

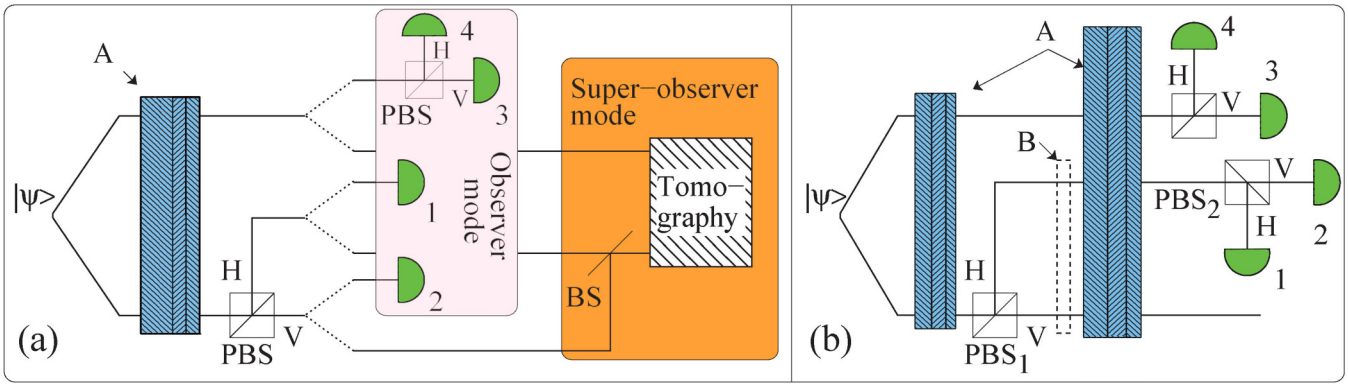

FIG. 2. (Color online) Scheme for the two experiments. (a) PaW experiment in "Observer" mode [left, pink (light gray) box] and "Super-observer" mode [right, orange(dark gray) box]. The experimenter in observer mode can prove the time evolution of the first photon (upper path) using only correlation measurements between it and the clock photon (lower path) without access to an external clock. The experimenter in super-observer mode [orange(dark gray) box] proves that the global state of the system is static through state tomography. (b) Two-time measurements in the GPPT mechanism. The two time measurements are represented by the two polarizing beam splitters PBS_1 and PBS_2, respectively. The blue (gray dashed) boxes (A) represent different thicknesses of birefringent plates which evolve the photons by rotating their polarization; different thicknesses represent different time evolutions. The PaW mechanism (a) is completely independent of the thickness, whereas the GPPT mechanism (b) allows it to be measured by the experimenter only through the clock photon (the abstract coordinate time is unaccessible and averaged away); the dashed box (B) represents a (known) phase delay of the clock photon only. PBS stands for polarizing beam splitter in the H/V basis; BS stands for beam splitter.

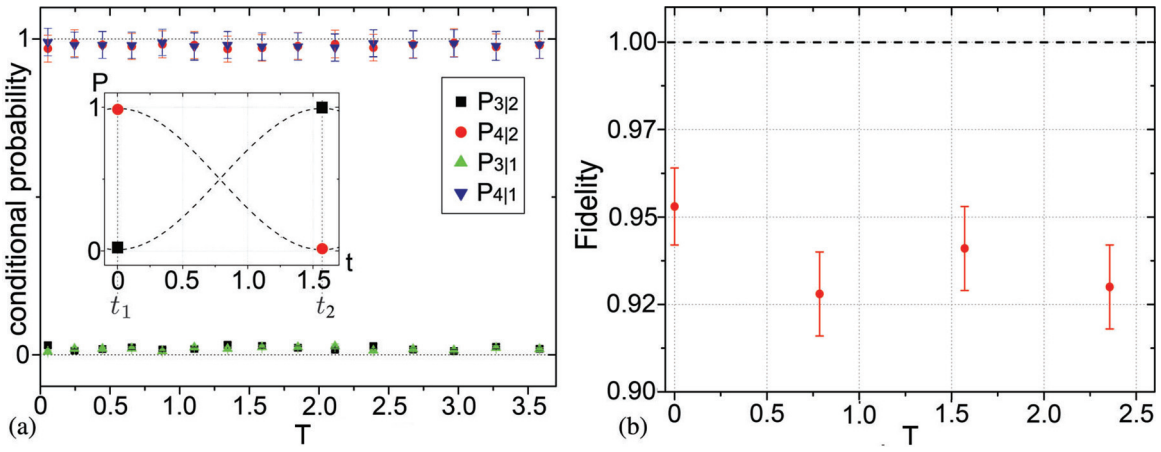

FIG. 3. (Color online) PaW experimental results. (a) Observer mode. Plot of the clock-time-dependent probabilities of measurement outcomes as a function of the optical plate thickness (corresponding to abstract coordinate time T). Downward triangles and squares represent $p(t_1) = P_{3|1}$ and $p(t_2) = P_{3|2}$, respectively, namely the probabilities of measuring V on the subsystem 1 as a function of the clock time t_1, t_2; upward triangles and circles represent $P_{4|1}$ and $P_{4|2}$, the probabilities of measuring H on the subsystem 1 as a function of the clock time. As expected from the PaW mechanism, these probabilities are independent of the abstract coordinate time T (dimensionless unit), represented by different phase plate A thicknesses (here we used a 957-μm-thick quartz plate rotated by 15 different equiseparated angles). The inset shows the graph that the observer himself would plot as a function of clock time; squares representing the probabilities of finding the system photon V at the two times t_1, t_2, the circles of finding it H. (b) Super-observer mode. Plot of the conditional fidelity between the tomographic reconstructed state and the theoretical initial state $|\Psi\rangle$ of Eq. (2) as a function of the abstract coordinate time T. The fact that the fidelity is constant and close to one (up to experimental imperfections) proves that the global entangled state is static.

a different phase plate A (of random thickness unknown to the experimenter) in every experimental run. In super-observer mode [Fig. 2(a), orange (dark gray) box] the experimenter takes the place of a hypothetical observer external to the universe that has access to the abstract coordinate time and tests whether the global state of the universe has any dependence on it. Hence, he must perform a quantum interference experiment that tests the coherence between the different histories (wave-function branches) corresponding to the different measurement outcomes of the internal observers, represented by the which-way information after the polarizing beam splitter PBS_1. In our setup, this interference is implemented by the beam splitter BS of Fig. 2(a) [orange (dark gray) box]. It is basically a quantum erasure experiment [19,20] that coherently "erases" the results of the time measurements of the internal observer; conditioned on the photon exiting from the right port of the beam splitter, the information on its input port (i.e., the outcome of the time measurement) is coherently erased [21]. The erasure of the time measurement by the internal observers is necessary to avoid having the external observer (super-observer) himself become correlated with the clock. However, the super-observer has access to abstract coordinate time; he knows the thickness of the blue plates, which is precluded to the internal observers, and he can test whether the global state evolves [experimental results for the super-observer mode are presented in Fig. 3(b)].

II. THE GPPT MECHANISM

In addition to the PaW mechanism, we also test the Gambini *et al.* (GPPT) proposal [12,16] for extending the PaW mechanism [9–11] to describe multiple time measurements. We start by describing this mechanism, and then relate it to our experimental setup.

Time-dependent measurements performed in the laboratory typically require two time measurements: they establish the times at which the experiment starts and ends, respectively. The PaW mechanism can accommodate the description of these situations by supposing that the state of the universe will contain records of the previous time measurements [11]. However, this observation in itself seems insufficient to derive the two-time correlation functions (transition probabilities and time propagators) with their required properties, a strong criticism directed to the PaW mechanism [2,11]. The GPPT proposal manages to overcome this criticism. It is composed of two main ingredients: the recourse to Rovelli's "evolving constants" to describe observables that commute with global constraints, and the averaging over the abstract coordinate time to eliminate any dependence on it in the observables. Our experiment illustrates only the latter aspect of the GPPT theory.

Measurements of a physical quantity at a given clock time, say t, are described by the conditional probability of obtaining an outcome on the system, say d, given that clock time measurement produces the outcome t. This conditional probability is given by [12,16]

$$p(d|t) = \frac{\int dT\ \mathrm{Tr}[P_{d,t}(T)\rho]}{\int dT\ \mathrm{Tr}[P_t(T)\rho]}, \tag{3}$$

where ρ is the global state, $P_t(T)$ is the projector relative to a result t for a clock measurement at coordinate time T, and $P_{d,t}(T)$ is the projector relative to a result d for a system measurement and t for a clock measurement at coordinate time T (working in the Heisenberg picture with respect to coordinate time T). Clearly, such expression can be readily generalized to arbitrary POVM measurements. (A similar expression, but in the Schrödinger picture, already appears in

[11].) The integral that averages over the abstract coordinate time T in (3) embodies the inaccessibility of the time T by the experimenter: he can access only the clock time t, an outcome of measurements on the clock system.

A generalization of this expression to multiple time measurements is expressed by [12]

$$p(d = d'|t_f, d_i, t_i) = \frac{\int dT \int dT' \, \mathrm{Tr}[P_{d',t_f}(T) P_{d_i,t_i}(T') \, \rho \, P_{d_i,t_i}(T')]}{\int dT \int dT' \, \mathrm{Tr}[P_{t_f}(T) P_{d_i,t_i}(T') \, \rho \, P_{d_i,t_i}(T')]}, \quad (4)$$

which gives the conditional probability of obtaining d' on the system given that the final clock measurement returns t_f and given that a "previous" joint measurement of the system and clock returns d_i, t_i. (This expression can also be formulated as a conventional state reduction driven by the first measurement [16].)

In our experiment to implement the GPPT mechanism [Fig. 2(b)] we must calculate the conditional probability that the system photon is V (namely detector 3 clicks) given that the clock photon is H after the first polarizing beam splitter PBS_1 (initial time measurement) and is H or V after the second polarizing beam splitter (final time measurement). The initial time measurement succeeds whenever one of photodetectors 1 or 2 click: This means that the clock photon chose the H path at PBS_1. (Our experiment discards the events where the first time measurement at PBS_1 finds V, although in principle one could easily take into account these cases by adding a polarizing beam splitter and two photodetectors also in the V output mode of PBS_1.) The final time measurement is given by the click either at photodetector 1 or 2; the clock dial shows $t_f = t_1$ and $t_f = t_2 = t_1 + \pi/2\omega$, respectively. Using the GPPT mechanism of Eq. (4), this means that the time-dependent probability that the system photon is vertical (detector 3 clicks) is given by

$$p(d = 3|t_f = t_k, d_i, t_i) = \frac{\int dT \int dT' \, \mathrm{Tr}[P_{d=3,t_f=t_k}(T) P_{d_i,t_i}(T') \rho P_{d_i,t_i}(T')]}{\int dT \int dT' \, \mathrm{Tr}[P_{t_f=t_k}(T) P_{d_i,t_i}(T') \rho P_{d_i,t_i}(T')]}, \quad (5)$$

where $P_{d=3,t_f=t_k}$ is the joint projector connected to detector 3 and detector $k = 1$ or $k = 2$ and P_{d_i,t_i} is the projector connected to the first time measurement. The latter projector is implemented in our experiment by considering only those events where either detector 1 or detector 2 clicks; this ensures that the clock photon chose the H path at PBS_1 (namely the initial time is t_i) and that the system photon was initialized as $|V\rangle$ at time t_i. (In principle, we could consider also a different initial time t_i' by employing also the events where the clock photons choose the path V at PBS_1.) Introducing the unitary abstract-time evolution operators U_T, the numerator of Eq. (5) becomes

$$\int dT \int dT' \, \mathrm{Tr}[P_{d=3,t_f=t_k} U_{T-T'} P_{d_i,t_i} \, U_{T'} \rho U_{T'}^\dagger P_{d_i,t_i} U_{T-T'}^\dagger] = \int dT \, \mathrm{Tr}[P_{d=3,t_f=t_k} U_T \, P_{d_i,t_i} \rho P_{d_i,t_i} U_T^\dagger],$$

where we use the property $U_T {U_{T'}}^\dagger = U_{T-T'}$ and we dropped one of the two time integrals by taking advantage of the time invariance of the global state ρ (which has been also tested experimentally in the super-observer mode). Gambini *et al.* typically suppose that the clock and the rest are in a factorized state [16], but this hypothesis is not strictly necessary for their theory [12]; we drop it so that we can use the same initial global state that we used for testing the PaW mechanism.

Using the same procedure also to calculate the denominator of Eq. (5), we can rewrite this equation as

$$p(d = 3|t_f = t_k, d_i, t_i) = \frac{\mathrm{Tr}[P_{d=3,t_f=t_k} \bar{\rho}]}{\mathrm{Tr}[P_{t_f=t_k} \bar{\rho}]}, \quad (6)$$

where $\bar{\rho}$ is the time average of the global state after the first projection, namely,

$$\bar{\rho} \propto \int dT \, U_T \rho_{t_i,d_i} U_T^\dagger, \quad \rho_{t_i,d_i} \equiv P_{d_i,t_i} \rho P_{d_i,t_i}, \quad (7)$$

where the averaging over the abstract coordinate time T is used to remove its dependence from the state. In our experiment such average is implemented by introducing random values of the phase plates A (unknown to the experimenter) in different experimental runs. In our GPPT experiment there are two possible values for the initial projector P_{d_i,t_i}: Either the clock photon is projected on the H path after PBS_1 (corresponding to an initial time t_i) or it is projected onto the V path (corresponding to an initial time $t_i + \pi/2\omega$). We will consider only the first case, which corresponds to a click of either detector 1 or 2: We are postselecting only on the experiments where the initial time is t_i. In this case, the global initial state will be $|H\rangle_c|V\rangle_r$ which is evolved into the vector $|\Psi(T)\rangle = [\cos(\omega(T+\tau))|H\rangle_c - \sin(\omega(T+\tau))|V\rangle_c][\cos\omega T|V\rangle_r + \sin\omega T|H\rangle_r]$ where τ is the time delay introduced by the plate B of Fig. 2(b), which represents a known clock delay introduced by the experimenter (as discussed below). Moreover, the projectors in Eq. (6) are

$$P_{d=3,t_f=t_k} \equiv |k\rangle_c\langle k| \otimes |V\rangle_r\langle V|, \text{ and}$$
$$P_{t_f=t_k} \equiv |k\rangle_c\langle k| \otimes \mathbb{1}_r, \quad (8)$$

where $|k=0\rangle_c \equiv |H\rangle_c$ and $|k=1\rangle_c \equiv |V\rangle_c$. The projector $P_{d=3,t_f=t_k}$ corresponds to the joint click of detectors k and 3, while $P_{t_f=t_k}$ corresponds to the click of detector k and either one of detectors 3 or 4. In other words, Eq. (6) can be written as

$$p(d = 3|t_f = t_k, d_i, t_i) = P_{3k}/(P_{3k} + P_{4k}), \quad (9)$$

where P_{jk} is the joint probability of detectors j and k clicking. For example, P_{32} is the joint probability that detector 3 and 2 click, namely that both the clock and the system photon were V. Considering only the component $|V\rangle_c|V\rangle_r$ of the state $|\Psi(T)\rangle$, this is given by

$$P_{32} = \frac{1}{2\pi}\int_0^{2\pi} d\varphi \sin^2(\varphi + \omega\tau)\cos^2\varphi = \frac{1 + 2\cos^2\omega\tau}{8}, \quad (10)$$

where we have calculated the integral over T of Eq. (7) using a change of variables $\omega T = \varphi$. Proceeding analogously for all the other joint probabilities, namely replacing the projectors (8) into (6), we find the probability for detector 3 clicking (namely the system photon being V) conditioned on the time

t_f read on the clock photon as

$$p(3|t_f = t_1) = (1 + 2\cos^2 \omega\tau)/4, \quad (11)$$

$$p(3|t_f = t_2) = (1 + 2\sin^2 \omega\tau)/4. \quad (12)$$

Summarizing, in our experiment [see Fig. 2(b)] the two-time measurements are implemented by the two polarizing beam splitters PBS_1 and PBS_2. PBS_1 represents the initial time measurement that determines when the experiment starts. It is a nondemolition measurement obtained by coupling the photon polarization to its propagation direction, while the initialization of the system state is here implemented through the entanglement. PBS_2 together with detectors 1 and 2 represents the final time measurement by determining the final polarization of the photon. Between these two time measurements both the system and the clock evolve freely (the evolution is implemented by the birefringent plates A). In the GPPT mechanism, the abstract coordinate time (the thickness of the quartz plates A) is inaccessible and must be averaged over [11,12,16]. This restriction is implemented in the experiment by avoiding having to take into account the thickness of the blue quartz plates A when extracting the conditional probabilities from the coincidence rates; the rates obtained with different plate thicknesses are all averaged together.

The time-dependent probability of finding the system photon vertically polarized is (as for the PaW mechanism described above) $p(t_1) = P_{3|1}$ and $p(t_2) = P_{3|2}$. However, a clock that returns only two possible values (t_1 and t_2) is not very useful. To obtain a more interesting clock, we can introduce a τ dependence in the expressions of these quantities by introducing varying time delays to the clock photon, implemented through quartz plates of variable thickness [dashed box B in Fig. 2(b)]. (Even though the experimenter has no access to abstract coordinate time, he can have access to systems that implement known time delays, that he can calibrate separately.) In this way, as detailed in Eqs. (11) and (12), he obtains a sequence of time-dependent values for the conditional probability: $p(t_1 + \tau_i) = (1 + 2\cos^2 \omega\tau_i)/4$ and $p(t_2 + \tau_i) = (1 + 2\sin^2 \omega\tau_i)/4$, where $\tau_i = \delta_i/\omega$ is the time delay of the clock photon obtained by inserting the quartz plate B with thickness δ_i in the clock photon path. The experimental results of the GPPT experiment are detailed in Fig. 4.

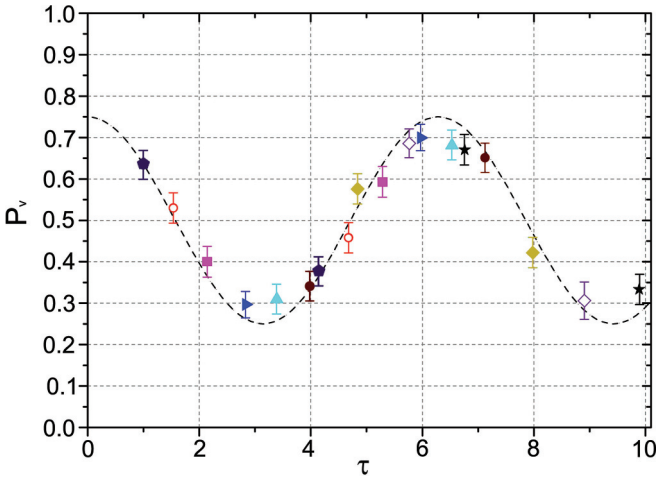

FIG. 4. (Color online) GPPT experimental results. Probability P_v that the upper photon is V as a function of the time τ (dimensionless unit) recovered from the lower photon. The points with matching colors and forms represent $p(t_1 + \tau_i)$ and $p(t_2 + \tau_i)$: blue pentagon, red circle, violet square, etc., for $i = 0,1,2,\ldots$, respectively. Here nine different values of τ_i are obtained from a thick quartz plate rotated by nine different angles. The dashed line is the theoretical value from Eq. (12). Since $t_2 = t_1 + \pi/2\omega$, we have plotted the points relative to $p(3|t_2)$ as displaced by $\pi/2$ with respect to the points relative to $p(3|t_1)$, so that the two curves (11) and (12) are superimposed in the graph.

III. EXPERIMENTAL SETUP

The experimental setup consists of two blocks: "preparation" and "measurement." The preparation block produces a singlet Bell state,

$$|\Psi\rangle = \frac{1}{\sqrt{2}}(|H\rangle_c|V\rangle_r - |V\rangle_c|H\rangle_r), \quad (13)$$

by exploiting the standard method of coherently superimposing the emission of two type I BBO crystals whose optical axes are rotated by 90°, nonpolarizing beam splitter, which is used to split the initial (collinear) biphoton field into two spatial modes c,r and an additional half-wave plate at 45° in the transmitted arm [22].

The measurement block can be mounted in different configurations corresponding to "observer" and "super-observer" ones of the PaW and GPPT schemes (Fig. 2). In general, each arm of the measurement block contains interference filters with central wavelength 702 nm [full width at half maximum (FWHM) 1 nm] and a polarizing beam splitter (PBS). Before the PBS the polarization of both photons evolves in the birefringent quartz plates A (blue boxes in Fig. 2) as $|V\rangle \to |V\rangle \cos\delta + i\,|H\rangle \sin\delta$, where δ is the material's optical thickness.

"Observer" mode in PaW scheme (Fig. 2, block a). In this mode, the polarization of the photon in the lower arm is used as a clock: The first polarizing beam splitter PBS_1 acts as a nondemolition measurement in the H/V basis of the polarization of the second photon, finally detected by single-photon avalanche diodes (SPADs) 1-2. In this mode, the experimenter has no access to an external clock; he can only use the correlations (coincidences) between detectors. The time-dependent probability of finding the first photon in $|V\rangle$ is obtained from the coincidence rate between detectors 3-1 (corresponding to a measurement at time t_1), or 3-2 (corresponding to a measurement at time t_2). Appropriately normalized, these coincidence rates yield the conditional probabilities $P_{3|x}$. The impossibility of directly accessing abstract coordinate time (the thickness of the plates) is implemented by averaging the coincidence rates obtained for all possible thicknesses of the birefringent plates A: The plate thickness does not enter into the data processing in any way. The corresponding experimental results are shown in Fig. 3(a).

"Super-observer" mode in PaW scheme (Fig. 2, block a). This mode is employed to prove that the global state is

static with respect to abstract coordinate time, represented by the thickness of the quartz plates A. The 50/50 beam splitter (BS) in block b performs a quantum erasure of the polarization measurement (performed by the polarizing beam splitter PBS_1) conditioned on the photon exiting its right port. For temporal stability, the interferometer is placed into a closed box. Iris diaphragms and narrow interference filters are used for spatial and frequency mode selection. The output state is reconstructed using ququart state tomography [23–25] (the two-photon polarization state lives in a four-dimensional Hilbert space), where the projective measurements are realized with polarization filters consisting of a sequence of quarter- and half-wave plates and a polarization prism which transmits vertical polarization (V). The fidelity between the tomographically reconstructed state and the theoretical state $|\Psi\rangle$ is reported in Fig. 3(b).

GPPT two-time scheme. Here a second PBS preceding detectors allows a two-time measurement. To obtain a more interesting time dependence we delay the clock photon with an additional birefringent plate B (dashed box in Fig. 2), a 1752-μm-thick quartz plate rotated at nine different angles, placed in the lower arm, and we repeat the same procedure described above for different thicknesses of plate B. This represents an internal observer that introduces a (known) time delay to his clock measurements. Our results are summarized in Fig. 4, where each color represents a different delay: the blue pentagon points refer to τ_0; the red circle points to τ_1, etc. They are in good agreement with the theory (dashed line). The reduction in visibility of the sinusoidal time dependence of the probability is caused by the decoherence effect due to the use of a low-resolution clock, a well-known effect [10,16,26,27].

IV. CONCLUSIONS

In conclusion, we presented two experimental setups. In the PaW setup, by running our experiment in two different modes ("observer" and "super-observer" mode) we have experimentally shown how the same entangled Hamiltonian eigenstate can be perceived as evolving by the internal observers that test the correlations between a clock subsystem and the rest (also when considering two-time measurements), whereas it is static for the super-observer that tests its global properties. In the GPPT setup we have shown one of the possible adaptations of the PaW mechanism to allow for multiple-time measurements. Our experiment is a practical implementation of the PaW and GPPT mechanisms but, obviously, it cannot discriminate between these and other proposed solutions for the problem of time [2–6]. In closing, we note that the time-dependent graphs of Fig. 4 have been obtained without any reference to an external time (or phase) reference, but only from measurements of correlations between the clock photon and the rest; they are an implementation of a "relational" measurement of a physical quantity (time) relative to an internal quantum reference frame [28,29].

ACKNOWLEDGMENTS

We thank A. Ashtekar for pointing out Ref. [12]. We acknowledge the Compagnia di San Paolo for support. This publication was made possible through the support of a grant from the John Templeton Foundation. E.V.M. acknowledges the Dynasty Foundation and the Russian Foundation for Basic Research (Project No. 13-02-01170-a).

[1] Saint Augustine, in *Confessions*, 2nd ed., edited by M. P. Foley (Hackett Publishing, Cambridge, MA, 2007), p. 17.
[2] K. V. Kuchař, in *Proceedings of the fourth Canadian Conference on General Relativity and Relativistic Astrophysics* (World Scientific, Singapore, 1992).
[3] C. J. Isham, in *Integrable Systems, Quantum Groups and Quantum Field Theories*, edited by L. A. Ibort and M. A. Rodríguez (Kluwer, Dordrecht, 1993).
[4] A. Ashtekar, New J. Phys. **7**, 198 (2005).
[5] E. Anderson, in *The Problem of Time in Quantum Gravity, Classical and Quantum Gravity: Theory, Analysis and Applications*, edited by V. R. Frignanni (Nova, New York, 2012).
[6] Z. Merali, Nature (London) **500**, 516 (2013).
[7] B. S. DeWitt, Phys. Rev. **160**, 1113 (1967).
[8] J. B. Hartle and S. W. Hawking, Phys. Rev. D **28**, 2960 (1983).
[9] D. N. Page and W. K. Wootters, Phys. Rev. D **27**, 2885 (1983).
[10] W. K. Wootters, Int. J. Theor. Phys. **23**, 701 (1984).
[11] D. N. Page, in *Physical Origins of Time Asymmetry*, edited by J. J. Halliwell *et al.* (Cambridge University Press, Cambridge, 1993).
[12] R. Gambini, R. A. Porto, J. Pullin, and S. Torterolo, Phys. Rev. D **79**, 041501(R) (2009).
[13] A. Peres, Am. J. Phys. **48**, 552 (1980).
[14] C. Rovelli, Int. J. Theor. Phys. **35**, 1637 (1996).
[15] W. G. Unruh and R. M. Wald, Phys. Rev. D **40**, 2598 (1989).
[16] R. Gambini, L. P. G. Pintos, and J. Pullin, Studies His. Philos. Mod. Phys. **42**, 256 (2011).
[17] C. Rovelli, Phys. Rev. D **43**, 442 (1991).
[18] A. Einstein, Ann. Phys. **17**, 891 (1905).
[19] M. O. Scully, B.-G. Englert, and H. Walther, Nature (London) **351**, 111 (1991).
[20] S. Dürr, T. Nonn, and G. Rempe, Nature (London) **395**, 33 (1998).
[21] J. Preskill, Lecture Notes for Physics **229**, 321 (1998).
[22] M. Genovese, Phys. Rep. **413**, 319 (2005).
[23] D. F. V. James, P. G. Kwiat, W. J. Munro, and A. G. White, Phys. Rev. A **64**, 052312 (2001).
[24] Yu. I. Bogdanov, G. Brida, M. Genovese, S. P. Kulik, E. V. Moreva, and A. P. Shurupov, Phys. Rev. Lett. **105**, 010404 (2010).
[25] Yu. I. Bogdanov, E. V. Moreva, G. A. Maslennikov, R. F. Galeev, S. S. Straupe, and S. P. Kulik, Phys. Rev. A **73**, 063810 (2006).
[26] R. Gambini, L. P. G. Pintos, and J. Pullin, Found. Phys. **40**, 93 (2010).
[27] I. L. Egusquiza, L. J. Garay, and J. M. Raya, Phys. Rev. A **59**, 3236 (1999).
[28] S. D. Bartlett, T. Rudolph, and W. Spekkens, Rev. Mod. Phys. **79**, 555 (2007).
[29] H. M. Wiseman, J. Opt. B: Quantum Semiclass. Opt. **6**, S849 (2004).